

Constraining the light Higgs bosons in the GNMSSM with recent Higgs data

Zhaoxia Heng, Zehan Li, Haijing Zhou

School of Physics, Henan Normal University, Xinxiang 453007, China

E-mail: zxheng@htu.edu.cn, hnuzehanli@163.com,
zhouhaijing0622@163.com

ABSTRACT: The search for light scalar and pseudoscalar particles provides a promising avenue for probing physics beyond the Standard Model (SM). In this study, we investigated the exotic decay channels of the 125 GeV SM-like Higgs boson into pairs of light CP-odd (a_s) or CP-even (h_s) Higgs bosons within the framework of the General Next-to-Minimal Supersymmetric Standard Model (GNMSSM). A comprehensive parameter space scan is performed using the MultiNest algorithm, incorporating constraints from HiggsSignals-2.6.2, HiggsBounds-5.10.2, and ATLAS experimental searches, under two distinct scenarios where either the lightest (h_1) or next-to-lightest (h_2) CP-even state is the observed Higgs boson (h). Our results demonstrate that HiggsBounds imposes the most stringent exclusion limits due to its sensitivity to direct searches for non-SM Higgs bosons. In the h_2 scenario, HiggsSignals can additionally exclude regions with suppressed exotic branching ratios (e.g., $Br(h \rightarrow a_s a_s \rightarrow \tau\tau bb) \leq 2.5\%$), due to its sensitivity to indirect deviations caused by the kinematically enhanced decay $h \rightarrow h_s h_s$. Under combined constraints from HiggsTools, h must retain at least 93% SM-like component ($V_h^{\text{SM}} \geq 0.93$) with no more than 32% singlet admixture ($V_h^{\text{S}} \leq 0.32$); in the h_2 case, the lightest scalar h_s exhibits high singlet purity ($V_{h_s}^{\text{S}} \geq 0.94$). Furthermore, dark matter (DM) phenomenology indicates that singlino- or higgsino-dominated DM is viable in the h_1 scenario, with dominant annihilation channels including $\tilde{\chi}_1^0 \tilde{\chi}_1^0 \rightarrow h_s a_s$ for singlino-like DM and chargino co-annihilation for higgsino-like DM, whereas the h_2 scenario favors higgsino-dominated DM.

Contents

1	Introduction	1
2	Theoretical preliminaries	3
2.1	Basics of the GNMSSM	3
2.2	Higgs sector of the GNMSSM	4
2.3	Neutralino sector of the GNMSSM	7
2.4	Trilinear Higgs couplings in the GNMSSM	8
3	Numerical result	8
3.1	Research strategy	8
3.2	HiggsTools constraints	10
3.3	Dark matter physics	15
4	Conclusion	17

1 Introduction

The discovery of the 125 GeV Higgs boson at the Large Hadron Collider (LHC) [1, 2] marked a milestone in particle physics because it confirmed the electroweak symmetry breaking (EWSB) mechanism described by the Standard Model (SM). However, the SM leaves several fundamental problems unsolved, such as the neutrino masses, hierarchy problem, and dark matter (DM) problem. These unresolved issues have motivated exploration of physics beyond the Standard Model (BSM), where extended Higgs sectors and new symmetries often predict additional scalar states.

Supersymmetry (SUSY) is a well-motivated candidate for BSM, providing solutions to the hierarchy problem and gauge coupling unification. The Minimum Supersymmetric Standard Model (MSSM) [3–6], as the most economical SUSY realization, has been extensively studied. However, it is challenged by DM constraints, the μ problem, the little hierarchy problem, and other issues. As a natural and minimal extension, the Next-to-Minimal Supersymmetric Standard Model (NMSSM) [7–9] introduces a gauge-singlet Higgs superfield. Its scalar component acquires a non-zero vacuum expectation value (vev), thereby generating an effective μ -term. Mixing between singlet and doublet superfields produces an additional CP-even Higgs (h_s) that mixes with MSSM-like states. This mixing can suppress the lightest Higgs mass while enabling the next-to-lightest Higgs to match the observed 125 GeV signal [10–16]. This scenario alleviates fine-tuning and offers rich phenomenology, including Higgs-to-Higgs decays [17–29] or exotic decays that involve neutralinos [30, 31].

Over the past decade, the NMSSM with the Z_3 -symmetric (Z_3 -NMSSM) [7–9] has drawn significant interest as a simple extension of the MSSM. However, experimental searches for light Higgs bosons, electroweakinos, and extra scalars have excluded a substantial portion of the theoretically natural parameter space, especially in regions where the 125 GeV Higgs mass, B-physics, and DM relic density are simultaneously satisfied [32, 33]. In addition, LHC searches for supersymmetric particles and tighter limits from DM direct detection experiments such as XENON-nT [34], PandaX-4T [35, 36], and LUX-ZEPLIN (LZ) [37, 38], have severely constrained the viable parameter space of the NMSSM. For large λ , predicted spin-independent scattering cross sections approach current experimental sensitivity [32, 33]; only scenarios with small λ or destructive cancellations can evade these bounds. However, small λ makes it difficult to achieve the correct Higgs mass without significant fine-tuning [32, 33]. Consequently, the Z_3 -NMSSM survives only in a narrow and fine-tuned region, challenging its original goal of solving the naturalness problem.

To address the aforementioned theoretical limitations of the Z_3 -NMSSM concerning the Higgs boson mass, the superparticle mass spectrum, and its connection to DM, researchers have proposed various extended frameworks, among which the General NMSSM (GNMSSM) [39–45] stands out as a representative example. By adding extra singlet couplings or Z_3 -symmetry-breaking terms, the GNMSSM enhances flexibility in the Higgs mass matrix and enables lighter CP-even and CP-odd states, which are consistent with LHC data [46]. In the framework of the GNMSSM, the lightest supersymmetric particle (LSP) serves as a viable DM candidate. Singlet-dominant particles such as singlino-dominated DM and singlet-dominated Higgs bosons, can form a secluded DM sector [42, 47]. In this sector, singlino-like DM primarily annihilates via the s-channel exchange of light CP-even or CP-odd Higgs bosons. The coupling strength between these scalar particles and DM governs both the DM relic abundance from the early universe and the scattering cross-section with nucleons in direct detection experiments. This connection establishes a link between collider physics and DM phenomenology, enabling constraints from high-energy and astrophysical observations to complement each other.

The couplings between these light Higgs bosons and SM fermions or gauge bosons are dynamically suppressed, leading to very low production rates in diphoton, ZZ, or WW channels. Consequently, these particles are difficult to detect with conventional search strategies. However, they can still appear indirectly through hidden-sector effects, especially via exotic Higgs decays. In parameter regions where the light Higgs bosons are lighter than half of the 125 GeV Higgs boson h , the latter can decay into pairs of such Higgs (e.g., $h \rightarrow h_s h_s$ or $a_s a_s$), each of which subsequently decays into b-jets, τ -lepton pairs, or other SM states. Although these cascade decays have small branching ratios, their low backgrounds make them sensitive probes for new physics. Meanwhile, the Higgs coupling to a light singlet scalar particle ($m_s < m_h/2$) drives a strong first-order electroweak phase transition (SFOEWPT) [48–51]. Therefore,

these light Higgs bosons are a compelling target for exotic Higgs decay searches at the LHC and future colliders. ATLAS and CMS have systematically searched for such signatures across multiple LHC runs, targeting final states such as $4b$ [52], $\mu\mu bb$ [53–55], $\tau\tau bb$ [56, 57], $\gamma\gamma\tau\tau$ [58], and 4μ [59–63].

This study investigates the $\tau\tau bb$ final state [57]. Compared with the $4b$ channel [52], this signature improves background suppression by exploiting the distinctive decay topology of the τ lepton, while retaining high signal efficiency. The `HiggsTools` package [64] is employed to constrain the model parameter space, identifying regions consistent with direct search limits and Higgs property measurements. Within the GNMSSM framework, we then examine the exotic decays $h \rightarrow h_s h_s / a_s a_s$ and evaluate their detectability. A preliminary analysis of DM properties in the allowed parameter region is also presented.

This paper is organized as follows. Section 2 introduces the GNMSSM framework and describes in detail its Higgs sector and the key trilinear Higgs couplings. Section 3 outlines our scanning strategy and the corresponding numerical results. Section 4 summarizes our conclusions.

2 Theoretical preliminaries

2.1 Basics of the GNMSSM

The GNMSSM extends the MSSM by introducing a gauge-singlet superfield \hat{S} that carries no baryon or lepton number. Consequently, the Higgs sector consists of the standard $SU(2)_L$ doublets $\hat{H}_u = (\hat{H}_u^+, \hat{H}_u^0)$ and $\hat{H}_d = (\hat{H}_d^0, \hat{H}_d^-)$, together with the singlet \hat{S} . Its gauge-invariant superpotential can be written as [8]:

$$W_{\text{GNMSSM}} = W_{\text{Yukawa}} + \lambda \hat{S} \hat{H}_u \cdot \hat{H}_d + \frac{\kappa}{3} \hat{S}^3 + \mu \hat{H}_u \cdot \hat{H}_d + \frac{1}{2} \mu' \hat{S}^2 + \xi \hat{S}, \quad (2.1)$$

where W_{Yukawa} contains the MSSM quark and lepton Yukawa interactions. The dimensionless couplings λ and κ govern the Higgs interactions, which are analogous to the Z_3 -NMSSM. The GNMSSM incorporates explicit Z_3 -symmetry-breaking via parameters μ , μ' and ξ . These terms resolve the inherent tadpole problem [8, 65] and cosmological domain-wall problem [66–68] in the Z_3 -NMSSM. Through a redefinition of the singlet field [69], the parameter ξ can be absorbed, allowing it to be set to zero without loss of generality. μ and μ' arise from the spontaneous breaking of discrete R -symmetries (\mathbb{Z}_4^R or \mathbb{Z}_8^R) at high scales [66, 69–72]. The inclusion of these explicit Z_3 -breaking terms modifies the neutral Higgs mass spectrum and generates markedly richer phenomenology than the Z_3 -NMSSM and MSSM.

2.2 Higgs sector of the GNMSSM

The soft SUSY-breaking terms in the Higgs sector of the GNMSSM can be expressed as:

$$-\mathcal{L}_{soft} = \left[\lambda A_\lambda S H_u \cdot H_d + \frac{1}{3} \kappa A_\kappa S^3 + m_3^2 H_u \cdot H_d + \frac{1}{2} m_S'^2 S^2 + \xi' S + h.c. \right] + m_{H_u}^2 |H_u|^2 + m_{H_d}^2 |H_d|^2 + m_S^2 |S|^2, \quad (2.2)$$

where H_u, H_d , and S are scalar components of the Higgs superfields, and $m_{H_u}^2, m_{H_d}^2$, and m_S^2 are their supersymmetry-breaking masses. After the electroweak symmetry breaking, the neutral components of the Higgs fields develop non-vanishing vevs:

$$\langle H_u^0 \rangle = \frac{v_u}{\sqrt{2}}, \quad \langle H_d^0 \rangle = \frac{v_d}{\sqrt{2}}, \quad \langle S \rangle = \frac{v_s}{\sqrt{2}}, \quad (2.3)$$

with $v = \sqrt{v_u^2 + v_d^2} \simeq 246$ GeV. Then, the Higgs sector is characterized by 11 independent physical parameters:

$$\tan \beta \equiv \frac{v_u}{v_d}, \quad \lambda, \quad \kappa, \quad v_s, \quad A_\lambda, \quad A_\kappa, \quad \mu, \quad \mu', \quad m_3^2, \quad m_S'^2, \quad \xi'. \quad (2.4)$$

To investigate the phenomenology of the Higgs sector, it is convenient to employ the following specialized parametrization:

$$\begin{aligned} H_{\text{NSM}} &\equiv \cos \beta \text{Re}(H_u^0) - \sin \beta \text{Re}(H_d^0), \\ H_{\text{SM}} &\equiv \sin \beta \text{Re}(H_u^0) + \cos \beta \text{Re}(H_d^0), \\ A_{\text{NSM}} &\equiv \cos \beta \text{Im}(H_u^0) - \sin \beta \text{Im}(H_d^0). \end{aligned} \quad (2.5)$$

In the basis of $(H_{\text{NSM}}, H_{\text{SM}}, \text{Re}[S])$, the mass matrix of CP-even Higgs fields can be written as: [42]

$$\begin{aligned} \mathcal{M}_{S,11}^2 &= \frac{\lambda v_s (\sqrt{2} A_\lambda + \kappa v_s + \sqrt{2} \mu') + 2m_3^2}{\sin 2\beta} + \frac{1}{2} (2m_Z^2 - \lambda^2 v^2) \sin^2 2\beta, \\ \mathcal{M}_{S,12}^2 &= -\frac{1}{4} (2m_Z^2 - \lambda^2 v^2) \sin 4\beta, \quad \mathcal{M}_{S,13}^2 = -\frac{\lambda v}{\sqrt{2}} (A_\lambda + \sqrt{2} \kappa v_s + \mu') \cos 2\beta, \\ \mathcal{M}_{S,22}^2 &= m_Z^2 \cos^2 2\beta + \frac{1}{2} \lambda^2 v^2 \sin^2 2\beta, \\ \mathcal{M}_{S,23}^2 &= \frac{\lambda v}{\sqrt{2}} \left[(\sqrt{2} \lambda v_s + 2\mu) - (A_\lambda + \sqrt{2} \kappa v_s + \mu') \sin 2\beta \right], \\ \mathcal{M}_{S,33}^2 &= \frac{(A_\lambda + \mu') \sin 2\beta}{2\sqrt{2} v_s} \lambda v^2 + \frac{\kappa v_s}{\sqrt{2}} (A_\kappa + 2\sqrt{2} \kappa v_s + 3\mu') - \frac{\mu}{\sqrt{2} v_s} \lambda v^2 - \frac{\sqrt{2}}{v_s} \xi' \end{aligned} \quad (2.6)$$

Similarly, based on $(A_{\text{NSM}}, \text{Im}[S])$, the mass matrix of CP-odd Higgs fields can be written as [42]

$$\mathcal{M}_{P,11}^2 = \frac{\lambda v_s (\sqrt{2} A_\lambda + \kappa v_s + \sqrt{2} \mu') + 2m_3^2}{\sin 2\beta}, \quad \mathcal{M}_{P,12}^2 = \frac{\lambda v}{\sqrt{2}} (A_\lambda - \sqrt{2} \kappa v_s - \mu'),$$

$$\begin{aligned} \mathcal{M}_{P,22}^2 &= \frac{(A_\lambda + 2\sqrt{2}\kappa v_s + \mu') \sin 2\beta}{2\sqrt{2}v_s} \lambda v^2 - \frac{\kappa v_s}{\sqrt{2}} (3A_\kappa + \mu') \\ &\quad - \frac{\mu}{\sqrt{2}v_s} \lambda v^2 - 2m_S'^2 - \frac{\sqrt{2}}{v_s} \xi'. \end{aligned} \quad (2.7)$$

The three CP-even mass eigenstates h_i ($i = 1, 2, 3$) and the two CP-odd Higgs mass eigenstates a_j ($j = 1, 2$) are obtained by diagonalizing the scalar (\mathcal{M}_S^2) and pseudoscalar (\mathcal{M}_P^2) mass matrices, respectively:

$$\begin{aligned} h_i &= V_{h_i}^{\text{NSM}} H_{\text{NSM}} + V_{h_i}^{\text{SM}} H_{\text{SM}} + V_{h_i}^{\text{S}} \text{Re}[S], \\ a_j &= V_{P,a_j}^{\text{NSM}} A_{\text{NSM}} + V_{P,a_j}^{\text{S}} \text{Im}[S]. \end{aligned} \quad (2.8)$$

For convenience, the mass of three CP-even states and two CP-odd states are ordered by increasing mass: $m_{h_1} < m_{h_2} < m_{h_3}$ and $m_{a_1} < m_{a_2}$. $|V_{h_i}^{\text{NSM}}|^2$, $|V_{h_i}^{\text{SM}}|^2$, and $|V_{h_i}^{\text{S}}|^2$ ($|V_{h_i}^{\text{NSM}}|^2 + |V_{h_i}^{\text{SM}}|^2 + |V_{h_i}^{\text{S}}|^2 = 1$) denote the composition ratios of the non-SM scalar component H_{NSM} , the SM component H_{SM} , and the singlet scalar component $\text{Re}[S]$ in the h_i , respectively. Similarly, $|V_{P,a_j}^{\text{NSM}}|^2$ and $|V_{P,a_j}^{\text{S}}|^2$ denote the composition ratios of the non-SM pseudoscalar component A_{NSM} and the singlet pseudoscalar component $\text{Im}[S]$ in the CP-odd mass eigenstate a_j , respectively. In terms of dominant components, the physical states are labeled as follows:

- h : the physical Higgs state with $|V_h^{\text{SM}}|^2 > 0.5$, corresponding to the SM-like Higgs boson.
- H, A_H : the CP-even and CP-odd non-SM-like Higgs states with $|V_H^{\text{NSM}}|^2 > 0.5$ and $|V_{P,A_H}^{\text{NSM}}|^2 > 0.5$, respectively.
- h_s, a_s : the scalar and pseudoscalar singlet-like Higgs states with $|V_{h_s}^{\text{S}}|^2 > 0.5$ and $|V_{P,a_s}^{\text{S}}|^2 > 0.5$, respectively.

The identity of the 125 GeV Higgs depends on the mass hierarchy:

- h_1 scenario: $h \equiv h_1$ with singlet-dominated h_s heavier ($m_{h_s} > m_h$)
- h_2 scenario: $h \equiv h_2$ with singlet-dominated h_s lighter ($m_h > m_{h_s}$)

In addition, the model predicts a pair of charged Higgs bosons:

$$H^\pm = \cos \beta H_u^\pm + \sin \beta H_d^\pm, \quad (2.9)$$

with the following mass: [8, 42]

$$m_{H^\pm}^2 = \frac{\lambda v_s (\sqrt{2}A_\lambda + \kappa v_s + \sqrt{2}\mu') + 2m_3^2}{\sin 2\beta} + m_W^2 - \frac{1}{2}\lambda^2 v^2. \quad (2.10)$$

To connect the theoretical inputs with experimental observables, we replaced the Lagrangian parameters $\mu, \mu', m_3^2, m_S'^2$, and ξ' with physical mass parameters:

- $m_A \equiv \sqrt{M_{P,11}^2}$: mass of a heavy MSSM-like CP-odd Higgs boson,
- $m_B \equiv \sqrt{M_{S,33}^2}$: mass of a CP-even singlet Higgs boson,
- $m_C \equiv \sqrt{M_{P,22}^2}$: mass of a CP-odd singlet Higgs boson,
- $\mu_{\text{tot}} \equiv \mu_{\text{eff}} + \mu$: higgsino mass parameter,
- $m_N \equiv \frac{2\kappa}{\lambda}\mu_{\text{eff}} + \mu'$: singlino mass parameter.

Then, the original Lagrangian parameters become:

$$\begin{aligned}
\mu &= \mu_{\text{tot}} - \frac{\lambda}{\sqrt{2}}v_s, & \mu' &= m_N - \sqrt{2}\kappa v_s, & m_3^2 &= \frac{m_A^2 \sin 2\beta}{2} - \lambda v_s \left(\frac{\kappa v_s}{2} + \frac{\mu'}{\sqrt{2}} + \frac{A_\lambda}{\sqrt{2}} \right), \\
\xi' &= \frac{v_s}{\sqrt{2}} \left[\frac{(A_\lambda + \mu') \sin 2\beta}{2\sqrt{2}v_s} \lambda v^2 + \frac{\kappa v_s}{\sqrt{2}} (A_\kappa + 2\sqrt{2}\kappa v_s + 3\mu') - \frac{\mu}{\sqrt{2}v_s} \lambda v^2 - m_B^2 \right], \\
m_S'^2 &= \frac{1}{2} \left[m_B^2 - m_C^2 + \lambda\kappa \sin 2\beta v^2 - 2\sqrt{2}\kappa v_s (A_\kappa + \frac{\kappa}{\sqrt{2}}v_s + \mu') \right].
\end{aligned} \tag{2.11}$$

This reparameterization simplifies the Higgs mass matrices (Eqs. 2.6, 2.7) to:

$$\begin{aligned}
\mathcal{M}_{S,11}^2 &= m_A^2 + \frac{1}{2}(2m_Z^2 - \lambda^2 v^2) \sin^2 2\beta, & \mathcal{M}_{S,12}^2 &= -\frac{1}{4}(2m_Z^2 - \lambda^2 v^2) \sin 4\beta, \\
\mathcal{M}_{S,13}^2 &= -\frac{\lambda v}{\sqrt{2}}(A_\lambda + m_N) \cos 2\beta, & \mathcal{M}_{S,22}^2 &= m_Z^2 \cos^2 2\beta + \frac{1}{2}\lambda^2 v^2 \sin^2 2\beta, \\
\mathcal{M}_{S,23}^2 &= \frac{\lambda v}{\sqrt{2}}[2\mu_{\text{tot}} - (A_\lambda + m_N) \sin 2\beta], & \mathcal{M}_{S,33}^2 &= m_B^2, \\
\mathcal{M}_{P,11}^2 &= m_A^2, & \mathcal{M}_{P,22}^2 &= m_C^2, & \mathcal{M}_{P,12}^2 &= \frac{\lambda v}{\sqrt{2}}(A_\lambda - m_N).
\end{aligned} \tag{2.12}$$

The neutral Higgs sector is fully specified by eight parameters: $\tan \beta$, λ , A_λ , m_A , m_B , m_C , m_N , and μ_{tot} . The remaining parameters (κ , A_κ , and v_s) exclusively govern triple Higgs couplings [42]. Considering the dominant radiative corrections from the top/stop loops to the mass of the SM-like Higgs boson, the mass of h can be approximated as [8, 10]

$$m_h^2 \simeq m_Z^2 \cos^2 2\beta + \frac{1}{2}\lambda^2 v^2 \sin^2 2\beta + \Delta^2 \tag{2.13}$$

with

$$\Delta^2 \simeq \frac{3m_t^4}{2\pi^2 v^2} \left[\ln \frac{M_S^2}{m_t^2} + \frac{X_t^2}{M_S^2} \left(1 - \frac{X_t^2}{12M_S^2} \right) \right] \tag{2.14}$$

where $M_S = \sqrt{m_{\tilde{t}_1} m_{\tilde{t}_2}}$, $m_{\tilde{t}_1}$ and $m_{\tilde{t}_2}$ are the masses of the two stop eigenstates, and $X_t = A_t - \mu_{\text{tot}} \cot \beta$.

In the light h_s scenario, the scalar mass matrix element $\mathcal{M}_{S,23}^2$ is parameterized as:

$$\mathcal{M}_{S,23}^2 = \sqrt{2}\lambda v \delta \mu_{\text{tot}} \quad (2.15)$$

where the dimensionless parameter $\delta \equiv [2\mu_{\text{tot}} - (A_\lambda + m_N) \sin 2\beta]/(2\mu_{\text{tot}})$ quantifies the cancellation between effective μ -term and SUSY-breaking contributions. This parametrization offers advantages: it naturally accommodates larger λ couplings while remaining compatible with LHC Higgs data through modest δ values. Thus, we used δ as an input parameter instead of A_λ in this work.

In the scenario with very heavy charged Higgs bosons, approximate expressions can be derived for the singlet-dominated states and their mixing parameters [73]:

$$\begin{aligned} m_{h_s}^2 &\simeq m_B^2 - \frac{\mathcal{M}_{S,13}^4}{m_A^2 - m_B^2}, & m_{a_s}^2 &\simeq m_C^2 - \frac{\mathcal{M}_{P,12}^4}{m_A^2 - m_C^2}, & \frac{V_{P,a_s}^{\text{NSM}}}{V_{P,a_s}^{\text{S}}} &= \frac{\mathcal{M}_{P,12}^2}{m_{a_s}^2 - m_A^2} \simeq 0, \\ \frac{V_h^{\text{S}}}{V_h^{\text{SM}}} &\simeq \frac{\mathcal{M}_{S,23}^2}{m_h^2 - m_B^2}, & V_h^{\text{NSM}} &\sim 0, & V_h^{\text{SM}} &\simeq \sqrt{1 - \left(\frac{V_h^{\text{S}}}{V_h^{\text{SM}}}\right)^2} \sim 1, \\ \frac{V_{h_s}^{\text{SM}}}{V_{h_s}^{\text{S}}} &\simeq \frac{\mathcal{M}_{S,23}^2}{m_{h_s}^2 - m_h^2}, & V_{h_s}^{\text{NSM}} &\sim 0, & V_{h_s}^{\text{S}} &\simeq \sqrt{1 - \left(\frac{V_{h_s}^{\text{SM}}}{V_{h_s}^{\text{S}}}\right)^2} \sim 1. \end{aligned} \quad (2.16)$$

These expressions indicate that $V_h^{\text{S}} \simeq -V_{h_s}^{\text{SM}}$ and that all scale with λ . In the limit of $\lambda \rightarrow 0$, the singlet fields decouple from the doublet Higgs fields, and the masses m_B , m_C , and m_N can be treated as the physical particle masses with high accuracy. Moreover, the singlet masses are independent and may assume small values, as they are only weakly constrained by current experimental data.

2.3 Neutralino sector of the GNMSSM

The interaction between gauginos and the fermionic components of the neutral Higgs bosons generates five neutralinos and two charginos, represented as $\tilde{\chi}_i^0$ ($i = 1, \dots, 5$) and $\tilde{\chi}_i^\pm$ ($i = 1, 2$), respectively. In the gauge eigenstate basis $\psi^0 = (-i\tilde{B}, -i\tilde{W}, \tilde{H}_d^0, \tilde{H}_u^0, \tilde{S})$, the corresponding symmetric neutralino mass matrix is given by [8]

$$M_{\tilde{\chi}^0} = \begin{pmatrix} M_1 & 0 & -m_Z \sin \theta_W \cos \beta & m_Z \sin \theta_W \sin \beta & 0 \\ & M_2 & m_Z \cos \theta_W \cos \beta & -m_Z \cos \theta_W \sin \beta & 0 \\ & & 0 & -\mu_{\text{tot}} & -\frac{1}{\sqrt{2}}\lambda v \sin \beta \\ & & & 0 & -\frac{1}{\sqrt{2}}\lambda v \cos \beta \\ & & & & m_N \end{pmatrix}, \quad (2.17)$$

where M_1 and M_2 denote the gaugino soft-breaking mass parameters, while $s_W \equiv \sin \theta_W$ and $c_W \equiv \cos \theta_W$. By diagonalization the mass matrix using the rotation matrix N , the physical neutralino mass eigenstates $\tilde{\chi}_i^0$ are obtained as follows:

$$\tilde{\chi}_i^0 = N_{i1}\psi_1^0 + N_{i2}\psi_2^0 + N_{i3}\psi_3^0 + N_{i4}\psi_4^0 + N_{i5}\psi_5^0, \quad (2.18)$$

where the index $i = 1, 2, \dots, 5$, arranged in ascending order of mass. The lightest neutralino, $\tilde{\chi}_1^0$, can serve as the DM candidate. In this state, $N_{13}^2 + N_{14}^2$ and N_{15}^2 correspond to the higgsino and singlino components of the physical state $\tilde{\chi}_1^0$, respectively. The lightest neutralino $\tilde{\chi}_1^0$ is classified as higgsino-dominated DM if $(N_{13}^2 + N_{14}^2) > 0.5$ and singlino-dominated DM if $N_{15}^2 > 0.5$. In scenarios where gauginos are significantly heavier and the condition $\mu_{tot}^2 - m_N^2 \gg \lambda^2 v^2$ holds, the mass of the singlino-dominated DM can be approximately given by [42]

$$m_{\tilde{\chi}_1^0} \simeq m_N + \frac{\lambda^2 v^2 (m_{\tilde{\chi}_1^0} - \mu_{tot} \sin 2\beta)}{2(m_{\tilde{\chi}_1^0}^2 - \mu_{tot}^2)} \simeq m_N \quad (2.19)$$

2.4 Trilinear Higgs couplings in the GNMSSM

For the light Higgs scenario in this study, we assumed a light CP-odd Higgs boson (a_1) that satisfies $2m_{a_1} < m_h$ to enable the exotic decay $h \rightarrow a_1 a_1$ (i.e. $h \rightarrow a_s a_s$) in both h_1 and h_2 scenarios. For the h_2 scenario, where the lightest CP-even Higgs boson h_1 is singlet-dominant, $h \rightarrow h_1 h_1$ (i.e., $h \rightarrow h_s h_s$) becomes accessible when $2m_{h_1} < m_h$. Both ATLAS and CMS collaborations have conducted searches for non-SM Higgs bosons (H , h_s , A_H and a_s), which established stringent exclusion bounds on key parameters such as the masses and relative couplings [74, 75].

The branching ratios of the exotic decays $h \rightarrow a_1 a_1$ and $h \rightarrow h_1 h_1$ are governed by their respective trilinear Higgs couplings $C_{ha_1 a_1}$ ($\equiv C_{ha_s a_s}$) and $C_{hh_1 h_1}$ ($\equiv C_{hh_s h_s}$). In the GNMSSM, these couplings are relevant to vacuum expectation values (v_u , v_d , v_s) and soft SUSY-breaking trilinear terms (A_λ , A_κ). While general analytic expressions for these couplings are provided in Ref. [18], the specific trilinear couplings relevant to our discussions are explicitly defined as follows [42]:

$$C_{hh_s h_s} = \lambda v V_h^{\text{SM}} V_{h_s}^{\text{S}} V_{h_s}^{\text{S}} (\lambda - \kappa \sin 2\beta) - \lambda \kappa v V_h^{\text{NSM}} V_{h_s}^{\text{S}} V_{h_s}^{\text{S}} \cos 2\beta + \sqrt{2} \kappa V_h^{\text{S}} V_{h_s}^{\text{S}} V_{h_s}^{\text{S}} (3m_N + A_\kappa) + C'_{h_s}(\lambda, \kappa, \tan \beta, v_s, A_\lambda, m_N), \quad (2.20)$$

$$C_{ha_s a_s} = \lambda v V_h^{\text{SM}} (\lambda + \kappa \sin 2\beta) + \lambda \kappa v V_h^{\text{NSM}} \cos 2\beta + \sqrt{2} \kappa V_h^{\text{S}} (m_N - A_\kappa) + C'_{a_s}(\lambda, \kappa, \tan \beta, v_s, A_\lambda, m_N), \quad (2.21)$$

where the last terms in the two equations, suppressed by Higgs mixings, depend on λ , κ , $\tan \beta$, v_s , A_λ and m_N .

3 Numerical result

3.1 Research strategy

We constructed the GNMSSM model file using SARAH [76–79], generated particle spectra with SPheno [76, 80–82], and used the parallelized MultiNest algorithm [83] to explore the parameter space. In the specific parameter space scan, we set the number of live points to $n_{\text{live}} = 8000$ and selected the GNMSSM parameter space

Parameter	Prior	Range	Parameter	Prior	Range
κ	Flat	-0.75–0.75	$\tan \beta$	Flat	5–60
λ	Flat	0–0.75	v_s/TeV	Flat	0.1–1.0
δ	Flat	-1.0–1.0	m_N/TeV	Flat	-1.0–1.0
m_B/GeV	Flat	1–300	m_C/GeV	Flat	1.0–300
A_t/TeV	Flat	1.0–3.0	$\mu_{\text{tot}}/\text{TeV}$	Flat	0.2–1.0
A_κ/TeV	Flat	-2.0–2.0			

Table 1. Parameter space explored in this study. All input parameters used flat distributions based on their unambiguous physical interpretations. Considering the substantial radiative corrections that the third-generation squark trilinear couplings (A_t and A_b) impose on the SM-like Higgs boson mass, we imposed $A_t = A_b$, where their magnitudes were treated as free variables. Non-critical SUSY-breaking parameters were fixed: $m_A = 2$ TeV, $M_1 = 1$ TeV, $M_2 = 2$ TeV, $M_3 = 3$ TeV. All parameters were defined at the renormalization scale $Q_{\text{input}} = 1$ TeV.

as shown in Table 1. The dimensionless coupling parameters λ and κ are mainly restricted to avoid a Landau singularity below the Grand Unified (GUT) scale [8], with λ restricted to the interval $[0, 0.75]$ and κ to $[-0.75, 0.75]$. The dimensionless parameter δ was varied over the range $[-1, 1]$ to enable a moderate cancellation between effective μ -term and SUSY-breaking contributions in the matrix element $\mathcal{M}_{S,23}^2$, as defined in Eq.(2.15). m_B and m_C denote the masses of the CP-even and CP-odd singlet Higgs bosons, respectively. To obtain a light CP-even or CP-odd Higgs boson, we set the mass bounds to $1 \text{ GeV} \leq m_B, m_C \leq 300 \text{ GeV}$. Due to the sizable radiative corrections from third-generation squark trilinear couplings A_t and A_b to the SM-like Higgs boson mass, we impose $A_t = A_b$, treat their magnitudes as free parameters, and vary A_t in the range of 1-3 TeV. Parameters m_N and μ_{tot} are the singlino and higgsino masses, respectively. Their scanning ranges covered a relatively broad neutralino mass spectrum. Parameters A_κ and v_s affect the triple Higgs couplings, and the selected scanning ranges enable a substantial variation in the Higgs self-coupling.

To improve scanning efficiency, the likelihood function used to guide the scan was defined as follows:

$$\mathcal{L} = \mathcal{L}_{\text{mass}} \times \mathcal{L}_{\text{HS}} \times \mathcal{L}_{\text{HB}} \times \mathcal{L}_{\text{B}} \quad (3.1)$$

where

- **Mass of the SM-like Higgs boson ($\mathcal{L}_{\text{mass}}$):** This constraint is satisfied when the mass of SM-like Higgs boson (either h_1 or h_2) lies within the range of 122 GeV to 128 GeV, accommodating theoretical and experimental uncertainties of approximately 3 GeV [84].

- **Higgs data fit (\mathcal{L}_{HS}):** The properties of the SM-like Higgs boson must be consistent with the combined LHC measurements at the 95% confidence level. A parameter point passes this constraint if the p -value computed by `HiggsSignals-2.6.2` [85–88] exceeds 0.05.
- **Extra Higgs searches (\mathcal{L}_{HB}):** All non-SM-like Higgs bosons are required to satisfy the 95% confidence level exclusion limits from direct searches at LEP, Tevatron, and the LHC, as evaluated by `HiggsBounds-5.10.2` [89–93]. A parameter point is accepted only if it passes all search channels.
- **B -physics observables (\mathcal{L}_{B}):** This constraint is satisfied when the theoretical predictions for the branching ratios of $B_s \rightarrow \mu^+\mu^-$ and $B \rightarrow X_s\gamma$ lie within the $\pm 2\sigma$ range of their respective experimental values [94].

Consequently, the likelihood $\mathcal{L} = 1$ only if all the above constraints are satisfied; otherwise, $\mathcal{L} = \exp(-100) \approx 0$. Our subsequent analysis is restricted to the parameter points with $\mathcal{L} = 1$.

In addition to the above basic constraints, we also incorporate constraints from `HiggsTools` [64], which integrates the updated versions of `HiggsBounds` and `HiggsSignals`. In `HiggsTools`, `HiggsBounds` provides direct constraints from extra scalar searches, whereas `HiggsSignals` assesses the compatibility with the observed 125 GeV Higgs properties.

3.2 HiggsTools constraints

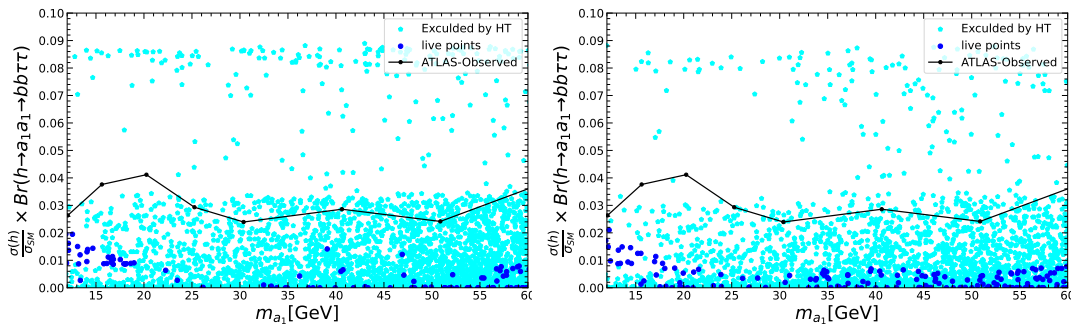


Figure 1. Surviving parameter samples after we applied the basic constraints in Sec. 3.1 were projected onto the plane of $\sigma(h)/\sigma_{SM}(h) \times Br(h \rightarrow a_1 a_1 \rightarrow bb\tau\tau)$ versus m_{a_1} . The blue points represent the surviving samples after further constraints by `HiggsTools` (HT); the black solid line denotes the ATLAS exclusion limit for the $h \rightarrow a_1 a_1 \rightarrow bb\tau\tau$ channel [57]. The left and right panels correspond to the h_1 and h_2 scenarios, respectively.

The direct search constraints for light Higgs bosons decaying into final states such as $4b$, $\mu\mu bb$ were primarily implemented within `HiggsTools`. To compare experimental

	h_1 scenario	h_2 scenario
live point	143	201
Excluded by both HB and HS	964	1021
Excluded only by HB	3287	2793
Excluded only by HS	32	42

Table 2. Numbers of surviving and excluded samples obtained with HiggsTools.

limitations on the parameter space in the light Higgs scenario, we projected the surviving samples that satisfied the basic constraints in Sec. 3.1 onto two-dimensional planes, where the vertical axes represent $\mu_{bb\tau\tau} \equiv \sigma(h)/\sigma_{\text{SM}}(h) \times \text{Br}(h \rightarrow a_1 a_1 \rightarrow bb\tau\tau)$, as shown in Figure 1. The left and right panels correspond to the h_1 and h_2 scenarios, respectively. The blue points represent the surviving samples after further constraints of HiggsTools. The ATLAS constraints [57] on the decay channel $h \rightarrow a_1 a_1 \rightarrow bb\tau\tau$ are applied (the solid line), and all parameter points above this limit are excluded. Figure 1 reveals that the upgraded HiggsTools imposes more stringent constraints than both the legacy HiggsSignals and HiggsBounds, as well as the ATLAS constraints on $h \rightarrow a_1 a_1 \rightarrow bb\tau\tau$. After the constraints from HiggsTools had been applied, the values of $\mu_{bb\tau\tau}$ could reach 1.9% in the h_1 scenario and 2.1% in the h_2 scenario.

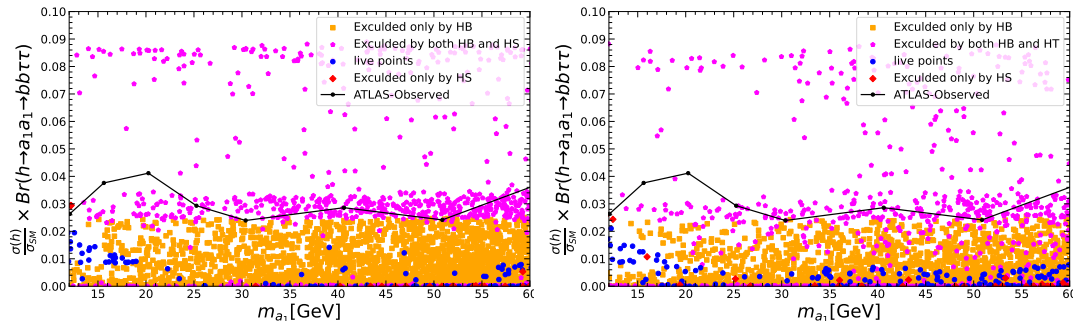


Figure 2. Parameter samples excluded by HiggsTools in Figure 1 are color-coded based on the exclusion source. The red diamond points denote samples that only HiggsSignals (HS) excludes, the orange square points denote samples that only HiggsBounds (HB) excludes, and the magenta pentagon points denote samples that both HB and HS exclude.

To compare the constraints from HiggsBounds and HiggsSignals on the GNMSSM parameter points in the light Higgs scenario, the parameter samples excluded by HiggsTools in Figure 1 are color-coded in Figure 2 based on the exclusion source. The red diamond markers represent samples excluded only by HiggsSignals, the orange square markers denote samples excluded only by HiggsBounds, and the magenta pentagon markers indicate samples excluded by both tools. Figure 2 shows that a small

number of parameter points are excluded by **HiggsSignals**, whereas the vast majority of such points are also excluded by **HiggsBounds**, indicating that **HiggsBounds** has stronger exclusion power. Table 2 shows a detailed summary of surviving and excluded samples obtained using **HiggsTools**. Approximately 96.7% (94.8%) of the parameter points were excluded by **HiggsTools** in the h_1 (h_2) scenario.

In the h_1 scenario, parameter points with relatively large values of $\text{Br}(h \rightarrow a_1 a_1 \rightarrow \tau\tau bb)$ —specifically, $\text{Br}(h \rightarrow a_1 a_1 \rightarrow \tau\tau bb) \geq 2.5\%$ —are excluded by both **HiggsSignals** and **HiggsBounds**. In contrast, points with smaller branching ratios are excluded only by **HiggsBounds**. This difference arises from the fact that **HiggsBounds** imposes direct constraints, whereas **HiggsSignals** imposes indirect constraints derived from precision measurements of the 125 GeV Higgs boson properties. Specifically, a sufficiently large branching ratio $\text{Br}(h \rightarrow a_1 a_1)$ can affect the properties of the 125 GeV Higgs boson and implies a large $\text{Br}(h \rightarrow a_1 a_1 \rightarrow \tau\tau bb)$, although the converse is not necessarily valid. Conversely, small values of $\text{Br}(h \rightarrow a_1 a_1 \rightarrow \tau\tau bb)$ always correspond to small $\text{Br}(h \rightarrow a_1 a_1)$, which has minimal impact on the 125 GeV Higgs boson properties.

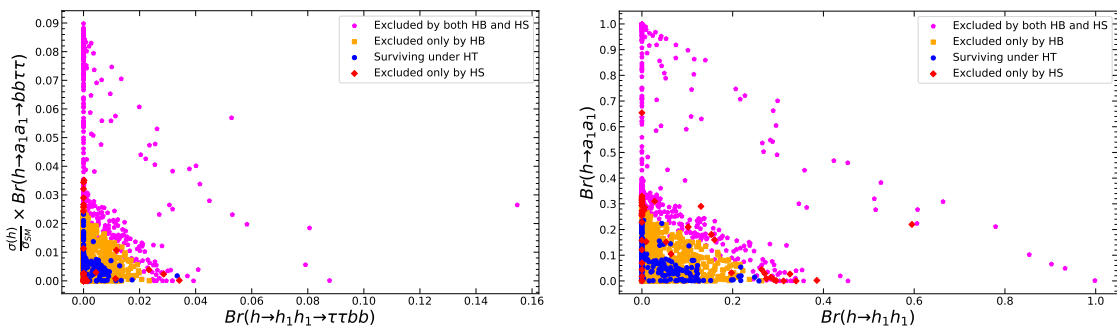


Figure 3. Following the right panel of Figure 2 in the h_2 scenario, the left panel here plots $\sigma(h)/\sigma_{SM}(h) \times \text{Br}(h \rightarrow a_1 a_1 \rightarrow bb\tau\tau)$ against $\text{Br}(h \rightarrow h_1 h_1 \rightarrow \tau\tau bb)$, and the right panel displays the relationship between $\text{Br}(h \rightarrow a_1 a_1)$ and $\text{Br}(h \rightarrow h_1 h_1)$.

The h_2 scenario shows characteristics similar to the h_1 scenario, but with distinct features. As shown in the right panel of Figure 2, some parameter points with $\text{Br}(h \rightarrow a_1 a_1 \rightarrow \tau\tau bb) \leq 2.5\%$ (indicated by magenta points) are excluded by **HiggsSignals**, since the exotic decay channel $h \rightarrow h_1 h_1$ becomes kinematically accessible in this scenario with an enhanced branching fraction. This enhancement may affect the properties of the SM-like Higgs boson and the constraints that **HiggsSignals** imposes. The left panel of Figure 3 shows the relationship between $\text{Br}(h \rightarrow a_1 a_1 \rightarrow \tau\tau bb)$ and $\text{Br}(h \rightarrow h_1 h_1 \rightarrow \tau\tau bb)$, and the right panel displays $\text{Br}(h \rightarrow a_1 a_1)$ versus $\text{Br}(h \rightarrow h_1 h_1)$ in the h_2 scenario. It reveals an anti-correlation between these branching ratios across the parameter space, which validates the proposed explanation. The right panel also indicates that the points featuring a relatively large $\text{Br}(h \rightarrow h_1 h_1)$ are predominantly excluded by the **HiggsSignals**.

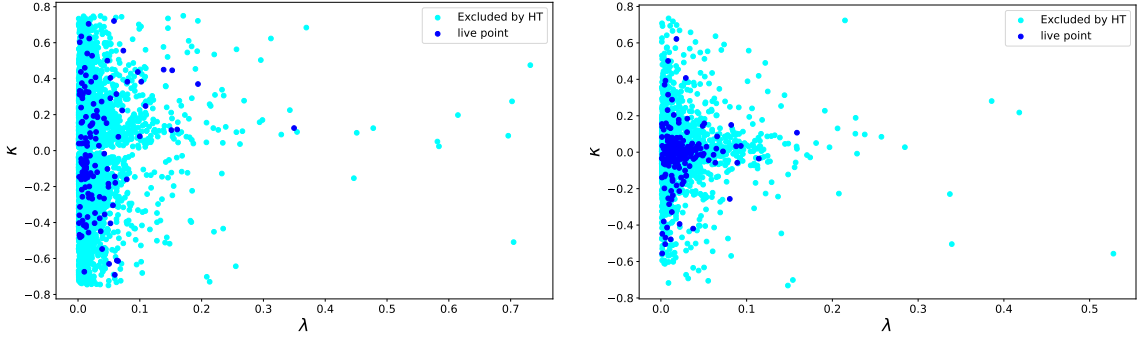


Figure 4. Relationship between parameters λ and κ , similar to Figure 1.

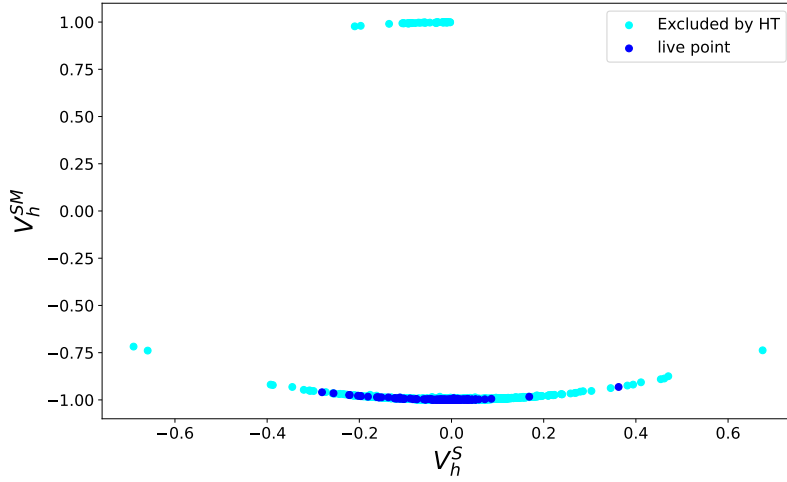


Figure 5. SM-like Higgs boson component in the h_1 scenario, similar to Figure 1.

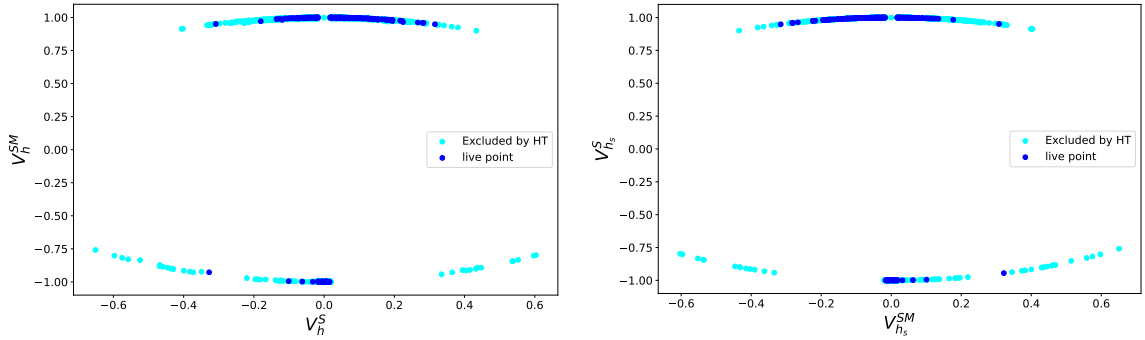


Figure 6. h_2 component (left panel) and h_1 component (right panel) in the h_2 scenario, similar to Figure 1.

The branching ratios for the exotic decays of $h \rightarrow a_1 a_1$ and $h \rightarrow h_1 h_1$ depend on the corresponding triple Higgs couplings $C_{ha_1 a_1}$ and $C_{hh_1 h_1}$, as defined in Eqs. (2.20) and (2.21). These couplings are determined primarily by parameters λ and κ , along with the SM-like fraction V_h^{SM} of the h boson. In the h_2 scenario, $C_{hh_1 h_1}$ is also mod-

ulated by the singlet fraction $V_{h_s}^S$ of the singlet-dominated state h_s . Figure 4 displays the correlation between λ and κ under **HiggsTools** constraints, which indicates that $\lambda \leq 0.1$ for most viable parameter points, which is consistent with experimental preferences for minimal doublet-singlet mixing. However, when λ is too small, the $\sim \lambda^2$ term in Eq. (2.13) has negligible contribution, and the calculation of the SM-like Higgs boson mass essentially reduces to that in the MSSM. The level of fine-tuning in this regime was comparable to that in the MSSM with no significant improvement. For benchmark point 4 in Table 4, with $m_{\tilde{t}_1} = 1952.2$ GeV and $m_{\tilde{t}_2} = 2071.5$ GeV, we found that achieving $m_h \simeq 125$ GeV resulted in $\Delta^2/m_h^2 \simeq 92\%$, which indicates a high degree of fine-tuning.

Figures 5 and 6 reveal the Higgs boson compositions. Both h_1 and h_2 scenarios require that the observed h boson is predominantly SM-like ($V_h^{\text{SM}} \geq 0.93$) with suppressed singlet admixture ($V_h^S \leq 0.32$). For the h_2 scenario, the lighter h_s state must exhibit high singlet purity ($V_{h_s}^S \geq 0.94$) and negligible SM-like components ($V_{h_s}^{\text{SM}} \leq 0.32$). Figure 6 further illustrates that $V_h^S \simeq -V_{h_s}^{\text{SM}}$, confirming the theoretical derivation presented in Eq.(2.16).

Point P1		Point P2	
Parameter	Value	Parameter	Value
$\lambda, \kappa,$	0.015, -0.369	λ, κ	0.017, -0.455
$\tan \beta, \delta$	41.5, 0.02	$\tan \beta, \delta$	37.6, 0.08
$v_s, \mu_{\text{tot}}, m_N$	212.8, 468.9, 23.6	$v_s, \mu_{\text{tot}}, m_N$	811.7, 342.0, 147.7
m_B, m_C	208.8, 144.6	m_B, m_C	181.6, 23.3
A_t, A_κ	2536.3, -685.3	A_t, A_κ	2592.3, -1152.8
Particle	Mass Spectrum	Particle	Mass Spectrum
$\tilde{\chi}_1^0, \tilde{\chi}_2^0, \tilde{\chi}_3^0$	23.5, 478.2, 483.5	$\tilde{\chi}_1^0, \tilde{\chi}_2^0, \tilde{\chi}_3^0$	146.5, 349.2, 354.2
$\tilde{\chi}_4^0, \tilde{\chi}_5^0$	1008.3, 2020.8	$\tilde{\chi}_4^0, \tilde{\chi}_5^0$	1008.1, 2020.8
$\tilde{\chi}_1^\pm, \tilde{\chi}_2^\pm$	481.4, 2021.1	$\tilde{\chi}_1^\pm, \tilde{\chi}_2^\pm$	352.2, 2021.0
h_s, h, H	154.8, 125.1, 2414.2	h_s, h, H	188.9, 125.3, 2273.6
a_s, A_H	48.0, 2414.1	a_s, A_H	16.6, 2273.6
Primary Decays	Branching Ratios [%]	Primary Decays	Branching Ratios [%]
$h \rightarrow b\bar{b}$	47.5	$h \rightarrow b\bar{b}$	49.4
$h \rightarrow W^+W^-$	22.4	$h \rightarrow W^+W^-$	24.0
$h \rightarrow a_s a_s$	16.1	$h \rightarrow a_s a_s$	11.9
Rotation Matrix	Element Value	Rotation Matrix	Element Value
$V_{h_s}^S, V_{h_s}^{\text{SM}}, V_h^S, V_h^{\text{SM}}$	-0.99996, 0.0005, -0.0003, -0.9997	$V_{h_s}^S, V_{h_s}^{\text{SM}}, V_h^S, V_h^{\text{SM}}$	-0.99996, -0.005, 0.005, -0.9996
$N_{11}, N_{12}, N_{13}, N_{14}, N_{15}$	0.0003, -0.0002, 0.0002, -0.0055, 0.99998	$N_{11}, N_{12}, N_{13}, N_{14}, N_{15}$	-0.00059, 0.0004, -0.004, 0.00997, -0.9999
$N_{21}, N_{22}, N_{23}, N_{24}, N_{25}$	-0.0599, 0.036, -0.71, 0.70, 0.004	$N_{21}, N_{22}, N_{23}, N_{24}, N_{25}$	0.048, -0.033, 0.71, -0.70, -0.00996
$N_{31}, N_{32}, N_{33}, N_{34}, N_{35}$	0.02, -0.02, -0.71, -0.71, -0.0037	$N_{31}, N_{32}, N_{33}, N_{34}, N_{35}$	-0.022, 0.023, 0.70, 0.71, 0.004
$N_{41}, N_{42}, N_{43}, N_{44}, N_{45}$	0.998, 0.0045, -0.028, 0.056, 0	$N_{41}, N_{42}, N_{43}, N_{44}, N_{45}$	-0.998, -0.004, 0.02, -0.05, 0
$N_{51}, N_{52}, N_{53}, N_{54}, N_{55}$	0.0019, -0.999, -0.01, 0.04, 0	$N_{51}, N_{52}, N_{53}, N_{54}, N_{55}$	0.002, -0.999, -0.0078, 0.04, 0
Primary Annihilation	Fraction [%]	Primary Annihilation	Fraction [%]
$\tilde{\chi}_1^0 \tilde{\chi}_1^0 \rightarrow b\bar{b}$	79.97	$\tilde{\chi}_1^0 \tilde{\chi}_1^0 \rightarrow h_s a_s$	81.2
$\tilde{\chi}_1^0 \tilde{\chi}_1^0 \rightarrow \tau^+ \tau^-$	19.74	$\tilde{\chi}_1^0 \tilde{\chi}_1^0 \rightarrow a_s a_s$	18.79
DM Observable	Value	DM Observable	Value
Ωh^2	0.000086	Ωh^2	0.001593
$\sigma_{p,n}^{\text{SI}}/(10^{-40} \text{cm}^2)$	6.8, 7.9	$\sigma_{p,n}^{\text{SI}}/(10^{-48} \text{cm}^2)$	4.1, 4.8
$\sigma_{p,n}^{\text{SD}}/(10^{-50} \text{cm}^2)$	2.5, 1.9	$\sigma_{p,n}^{\text{SD}}/(10^{-48} \text{cm}^2)$	3.6, 2.8

Table 3. Benchmark points P1 and P2 compatible with all experimental constraints. Both points correspond to singlino-dominated DM in the h_1 scenario. All mass parameters are given in GeV.

Point P3		Point P4	
Parameter	Value	Parameter	Value
$\lambda, \kappa,$	0.16, 0.117	λ, κ	0.026, -0.016
$\tan \beta, \delta$	20.4, -0.02	$\tan \beta, \delta$	23.7, 0.108
$v_s, \mu_{\text{tot}}, m_N$	739.4, 269.5, 776.5	$v_s, \mu_{\text{tot}}, m_N$	872.6, 405.6, -655.4
m_B, m_C	282.3, 240.0	m_B, m_C	51.2, 73.5
A_t, A_κ	2694.0, -1683.3	A_t, A_κ	2720.2, 1859.9
Particle	Mass Spectrum	Particle	Mass Spectrum
$\tilde{\chi}_1^0, \tilde{\chi}_2^0, \tilde{\chi}_3^0$	273.8, 279.6, 777.0	$\tilde{\chi}_1^0, \tilde{\chi}_2^0, \tilde{\chi}_3^0$	413.0, 418.1, 655.4
$\tilde{\chi}_4^0, \tilde{\chi}_5^0$	1008.1, 2020.8	$\tilde{\chi}_4^0, \tilde{\chi}_5^0$	1008.2, 2020.7
$\tilde{\chi}_1^\pm, \tilde{\chi}_2^\pm$	277.3, 2021.0	$\tilde{\chi}_1^\pm, \tilde{\chi}_2^\pm$	416.1, 2021.0
h_s, h, H	169.1, 125.3, 2104.7	h_s, h, H	21.77, 125.4, 2177.9
a_s, A_H	61.2, 2103.9	a_s, A_H	56.8, 2177.9
Primary Decays	Branching Ratios [%]	Primary Decays	Branching Ratios [%]
$h \rightarrow b\bar{b}$	52.1	$h \rightarrow b\bar{b}$	48.4
$h \rightarrow W^+W^-$	24.0	$h \rightarrow W^+W^-$	23.7
$h \rightarrow a_s a_s / h_s h_s$	8.8/0	$h \rightarrow a_s a_s / h_s h_s$	3.6/9.96
Rotation Matrix	Element Value	Rotation Matrix	Element Value
$V_{h_s}^S, V_{h_s}^{SM}, V_h^S, V_h^{SM}$	-0.999, 0.03, -0.03, -0.998	$V_{h_s}^S, V_{h_s}^{SM}, V_h^S, V_h^{SM}$	0.9997, -0.021, 0.021, 0.9989
$N_{11}, N_{12}, N_{13}, N_{14}, N_{15}$	0.044, -0.033, 0.71, -0.70, 0.037	$N_{11}, N_{12}, N_{13}, N_{14}, N_{15}$	0.054, -0.035, 0.71, -0.70, -0.0029
$N_{21}, N_{22}, N_{23}, N_{24}, N_{25}$	-0.023, 0.023, 0.70, 0.71, 0.019	$N_{21}, N_{22}, N_{23}, N_{24}, N_{25}$	0.021, -0.022, -0.71, -0.71, 0.014
$N_{31}, N_{32}, N_{33}, N_{34}, N_{35}$	-0.0001, 0.0009, -0.04, 0.01, 0.999	$N_{31}, N_{32}, N_{33}, N_{34}, N_{35}$	-0.0001, 0.0002, 0.012, 0.0078, 0.999899
$N_{41}, N_{42}, N_{43}, N_{44}, N_{45}$	-0.9987, -0.004, 0.015, -0.047, 0.001	$N_{41}, N_{42}, N_{43}, N_{44}, N_{45}$	-0.998, -0.004, 0.02, -0.05, 0
$N_{51}, N_{52}, N_{53}, N_{54}, N_{55}$	-0.002, 0.999, 0.007, -0.039, -0.0001	$N_{51}, N_{52}, N_{53}, N_{54}, N_{55}$	0.002, -0.999, -0.0098, 0.04, 0
Primary Annihilation	Fraction [%]	Primary Annihilation	Fraction [%]
$\tilde{\chi}_1^0 \tilde{\chi}_1^\pm \rightarrow d\bar{u}/\bar{d}u$	10.58	$\tilde{\chi}_1^0 \tilde{\chi}_1^\pm \rightarrow d\bar{u}/\bar{d}u$	10.05
$\tilde{\chi}_1^0 \tilde{\chi}_1^\pm \rightarrow s\bar{c}/\bar{s}c$	10.58	$\tilde{\chi}_1^0 \tilde{\chi}_1^\pm \rightarrow s\bar{c}/\bar{s}c$	10.05
$\tilde{\chi}_1^0 \tilde{\chi}_1^\pm \rightarrow b\bar{t}/\bar{t}b$	7.8	$\tilde{\chi}_1^0 \tilde{\chi}_1^\pm \rightarrow b\bar{t}/\bar{t}b$	6.66
$\tilde{\chi}_1^0 \tilde{\chi}_1^0 \rightarrow W^+W^-$	6.7	$\tilde{\chi}_1^0 \tilde{\chi}_1^0 \rightarrow W^+W^-$	4.84
$\tilde{\chi}_1^0 \tilde{\chi}_1^0 \rightarrow ZZ$	5.21	$\tilde{\chi}_2^0 \tilde{\chi}_1^\pm \rightarrow d\bar{u}/\bar{d}u$	4.41
$\tilde{\chi}_1^0 \tilde{\chi}_1^\pm \rightarrow e\bar{\nu}_e/\bar{\nu}_e e$	3.53	$\tilde{\chi}_2^0 \tilde{\chi}_1^\pm \rightarrow s\bar{c}/\bar{s}c$	4.41
$\tilde{\chi}_1^0 \tilde{\chi}_1^\pm \rightarrow \mu\bar{\nu}_\mu/\bar{\nu}_\mu \mu$	3.53	$\tilde{\chi}_1^0 \tilde{\chi}_1^0 \rightarrow ZZ$	3.81
$\tilde{\chi}_1^0 \tilde{\chi}_1^\pm \rightarrow \tau\bar{\nu}_\tau/\bar{\nu}_\tau \tau$	3.50	$\tilde{\chi}_1^0 \tilde{\chi}_1^\pm \rightarrow e\bar{\nu}_e/\bar{\nu}_e e$	3.35
$\tilde{\chi}_2^0 \tilde{\chi}_1^\pm \rightarrow d\bar{u}/\bar{d}u$	3.17	$\tilde{\chi}_1^0 \tilde{\chi}_1^\pm \rightarrow \mu\bar{\nu}_\mu/\bar{\nu}_\mu \mu$	3.35
$\tilde{\chi}_2^0 \tilde{\chi}_1^\pm \rightarrow s\bar{c}/\bar{s}c$	3.17	$\tilde{\chi}_1^0 \tilde{\chi}_1^\pm \rightarrow \tau\bar{\nu}_\tau/\bar{\nu}_\tau \tau$	3.27
DM Observable	Value	DM Observable	Value
Ωh^2	0.0091	Ωh^2	0.02
$\sigma_{p,n}^{\text{SI}}/(10^{-48}\text{cm}^2)$	6.32, 5.47	$\sigma_{p,n}^{\text{SI}}/(10^{-48}\text{cm}^2)$	1.78, 4.85
$\sigma_{p,n}^{\text{SD}}/(10^{-43}\text{cm}^2)$	1.64, 1.26	$\sigma_{p,n}^{\text{SD}}/(10^{-43}\text{cm}^2)$	4.08, 3.13

Table 4. Benchmark points P3 and P4 that satisfy all experimental constraints. Points P3 and P4 represent higgsino-dominated DM in the h_1 and h_2 scenarios, respectively. All mass parameters are given in GeV.

3.3 Dark matter physics

To further elucidate the DM phenomenology in the light Higgs scenario of the GN-MSSM parameter space, the package MicrOMEGAs [95–101] was used to calculate the DM relic density and the spin-dependent (SD) and spin-independent (SI) DM-nucleon cross sections. It was assumed that a large DM population existed in the early universe and froze out to match the current Planck observation, $\Omega_{\text{DM}} h^2 = 0.12 \pm 0.01$ [102]. In this study, the relic density of DM (the lightest neutralino $\tilde{\chi}_1^0$) was required to be below the central value of 0.12. The SI and SD cross sections were scaled by a factor of $\Omega h^2/0.12$. It was found that in the h_1 scenario, the DM can be either singlino- or higgsino-dominated, whereas in the h_2 scenario, it

is higgsino-dominated.

Four benchmark points, listed in Tables 3 and 4, were selected based on their dominant annihilation processes. These points satisfy the latest direct detection constraints from LZ-2024 [38]. Imposing these constraints results in generally small values of the parameter λ . Within the h_1 scenario, points P1 and P2 correspond to singlino-dominated DM, for which the mass satisfies $m_{\tilde{\chi}_1^0} \simeq m_N$, consistent with Eq.(2.19). The dominant annihilation channels differ markedly between P1 and P2. For point P1 with $m_{\tilde{\chi}_1^0} = 23.5$ GeV, the dominant DM annihilation channels are $\tilde{\chi}_1^0 \tilde{\chi}_1^0 \rightarrow b\bar{b}/\tau^+\tau^-$. In contrast, for point P2, $m_{\tilde{\chi}_1^0} = 146.5$ GeV, the condition $2m_{\tilde{\chi}_1^0} > m_{h_s} + m_{a_s}$ is satisfied. This opens the kinematically allowed channel $\tilde{\chi}_1^0 \tilde{\chi}_1^0 \rightarrow h_s a_s$, which becomes the predominant annihilation mode. This process proceeds via s -channel exchange of CP-odd Higgs bosons and t -channel exchange of neutralinos. Given that the contributions from the exchanges of a_s and $\tilde{\chi}_1^0$ are dominant for the small λ and sizable $|\kappa|$, the thermally averaged annihilation cross section $\langle\sigma v\rangle$ can be simplified as follows [73]:

$$\langle\sigma v\rangle \simeq \frac{1}{64\pi m_{\tilde{\chi}_1^0}^2} \left\{ \left[1 - \frac{(m_{h_s} + m_{a_s})^2}{4m_{\tilde{\chi}_1^0}^2} \right] \left[1 - \frac{(m_{h_s} - m_{a_s})^2}{4m_{\tilde{\chi}_1^0}^2} \right] \right\}^{1/2} |\mathcal{A}_s + \mathcal{A}_t|^2,$$

where the s - and t -channel contributions are approximated by

$$\begin{aligned} \mathcal{A}_s &\simeq \frac{-2m_{\tilde{\chi}_1^0} C_{\tilde{\chi}_1^0 \tilde{\chi}_1^0 a_s} C_{h_s a_s a_s}}{m_{a_s}^2 - 4m_{\tilde{\chi}_1^0}^2}, \\ \mathcal{A}_t &\simeq -2C_{\tilde{\chi}_1^0 \tilde{\chi}_1^0 h_s} C_{\tilde{\chi}_1^0 \tilde{\chi}_1^0 a_s} \left[1 + \frac{2m_{a_s}^2}{4m_{\tilde{\chi}_1^0}^2 - (m_{h_s}^2 + m_{a_s}^2)} \right], \end{aligned} \quad (3.2)$$

respectively. In the small- λ case, $C_{\tilde{\chi}_1^0 \tilde{\chi}_1^0 h_s} \simeq C_{\tilde{\chi}_1^0 \tilde{\chi}_1^0 a_s} \simeq -\sqrt{2}\kappa$, $C_{h_s a_s a_s} \simeq \sqrt{2}\kappa(m_N - A_\kappa)$ [42]. For point P2, $|(m_N - A_\kappa)m_{\tilde{\chi}_1^0}| \ll (4m_{\tilde{\chi}_1^0}^2 - m_{a_s}^2)$. Therefore, the t -channel contributed much more than that from the s -channel, which indicates that the t -channel contribution is dominant. Additionally, the channel $\tilde{\chi}_1^0 \tilde{\chi}_1^0 \rightarrow a_s a_s$ is also open, proceeding through s -channel CP-even Higgs exchange and t -channel neutralino exchange.

Benchmark points P3 and P4 shown in Table 4 represent higgsino-dominated DM in scenarios h_1 and h_2 , respectively. For both points, $N_{13}^2 + N_{14}^2 \simeq 0.994$, which indicates that the DM composition is very close to the pure higgsino limit. Table 4 also reveals that the masses of the lightest neutralino, next-to-lightest neutralino, and lightest chargino are nearly degenerate. The dominant annihilation channels mainly proceed via co-annihilation processes $\tilde{\chi}_i^0 \tilde{\chi}_1^\pm \rightarrow XY$ ($i = 1, 2$) and annihilation channels $\tilde{\chi}_1^0 \tilde{\chi}_1^0 \rightarrow W^+W^-/ZZ$, where X and Y denote the SM quarks or leptons. The effective annihilation cross-section can be written as [103]

$$\sigma_{eff} = \sum_{ij} \sigma(\tilde{\chi}_i \tilde{\chi}_j \rightarrow XY) \times \frac{g_i g_j}{g_{eff}^2} (1 + \Delta_i)^{3/2} (1 + \Delta_j)^{3/2} \exp[-x(\Delta_i + \Delta_j)] \quad (3.3)$$

where $\Delta_i \equiv (m_{\tilde{\chi}_i} - m_{\tilde{\chi}_1^0})/m_{\tilde{\chi}_1^0}$, $x \equiv m_{\tilde{\chi}_1^0}/T$ (with T being the temperature), g_i is the number of degrees of freedom for $\tilde{\chi}_i$, and

$$g_{eff} \equiv \sum_{i=1}^N g_i (1 + \Delta_i)^{3/2} \exp(-x\Delta_i). \quad (3.4)$$

Thus, the relic density was primarily determined by the mass splitting among higgsino-like particles.

Given the complexity of DM physics and its close relation to Higgs phenomenology, a detailed study of DM properties, particularly in the light Higgs scenario, will be the focus of future work.

4 Conclusion

This study investigated the exotic decay of the SM-like Higgs boson into pairs of the lightest CP-odd or CP-even Higgs bosons within the framework of GNMSSM. A comprehensive scan of the parameter space was first conducted using the MultiNest algorithm, subject to experimental constraints from `HiggsSignals-2.6.2` and `HiggsBounds-5.10.2`. To assess the implications of recent Higgs precision measurements for light Higgs scenarios (both $h_1 = h$ and $h_2 = h$ scenarios), we separately examined the exclusion limits provided by `HiggsSignals` and the `HiggsBounds` implementation in `HiggsTools`. Within the phenomenologically allowed parameter region, we further conducted a preliminary analysis of DM properties. The main findings were summarized as follows:

- In both the h_1 and h_2 scenarios, `HiggsBounds` imposes the most stringent constraints on the theoretical parameter space. In contrast, `HiggsSignals` and individual ATLAS searches exhibit comparatively weaker constraining power; moreover, the vast majority of parameter points excluded by these analyses are also disfavored by `HiggsBounds`. This is because `HiggsBounds` provides direct constraints from dedicated searches for non-SM Higgs bosons, whereas `HiggsSignals` derives indirect constraints based on global compatibility with experimental data.
- Notably, the analysis of the h_2 scenario reveals unique phenomenological features. Specifically, `HiggsSignals` can exclude certain parameter points with relatively low exotic decay rates, especially when $Br(h \rightarrow a_1 a_1 \rightarrow \tau\tau bb) \leq 2.5\%$. This exclusion effect stems from the kinematic accessibility of the $h_2 \rightarrow h_1 h_1$ decay process, which has a significantly enhanced branching ratio. Such enhanced decays will modify the properties of the SM-like Higgs boson, thereby increasing the sensitivity of `HiggsSignals` to indirect constraints in regions where they were previously suppressed due to kinematic factors.

- Under the combined constraints of **HiggsTools**, both h_1 and h_2 scenarios require that the observed h boson is predominantly SM-like ($V_h^{\text{SM}} \geq 0.93$) with minimal singlet admixture ($V_h^{\text{S}} \leq 0.32$). In the h_2 scenario, the lighter h_s state must exhibit high singlet purity ($V_{h_s}^{\text{S}} \geq 0.94$) and negligible SM-like components ($V_{h_s}^{\text{SM}} \leq 0.32$).
- In the h_1 scenario, DM can be either singlino- or higgsino-dominated, whereas in the h_2 scenario, it is higgsino-dominated. For higgsino-dominated DM, mostly annihilation channels of DM are achieved through co-annihilation with chargino; For singlino-dominated DM, mostly annihilation channels of DM may be $\tilde{\chi}_1^0 \tilde{\chi}_1^0 \rightarrow h_s a_s$.

Despite constraints from current Higgs data on light Higgs scenarios, phenomenologically viable regions in the parameter space persist. These regions merit further investigation for two principal reasons. First, DM physics exhibits considerable complexity and is deeply intertwined with Higgs phenomenology. Second, the singlet light Higgs spectrum can induce a SFOEWPT in the early universe [104, 105]. This mechanism satisfies the necessary conditions for electroweak baryogenesis (EWBG), providing a plausible explanation for the observed baryon asymmetry of the universe, and simultaneously produces detectable gravitational wave (GW) signals during the phase transition. These aspects will form the core focus of our future work.

Acknowledgement

We sincerely thank Prof. Junjie Cao for helpful discussions. We thank LetPub [106] for its linguistic assistance during the preparation of this manuscript. This work was supported by the National Natural Science Foundation of China (Grant No. 12505122) and the Natural Science Foundation of Henan Province (Grant No. 252300423511).

References

- [1] ATLAS collaboration, G. Aad et al., *Combined search for the Standard Model Higgs boson using up to 4.9 fb^{-1} of pp collision data at $\sqrt{s} = 7 \text{ TeV}$ with the ATLAS detector at the LHC*, *Phys. Lett. B* **710** (2012) 49 [1202.1408].
- [2] CMS collaboration, S. Chatrchyan et al., *Combined results of searches for the standard model Higgs boson in pp collisions at $\sqrt{s} = 7 \text{ TeV}$* , *Phys. Lett. B* **710** (2012) 26 [1202.1488].
- [3] H. P. Nilles, *Supersymmetry, Supergravity and Particle Physics*, *Phys. Rept.* **110** (1984) 1.

- [4] H. E. Haber and G. L. Kane, *The Search for Supersymmetry: Probing Physics Beyond the Standard Model*, *Phys. Rept.* **117** (1985) 75.
- [5] J. F. Gunion and H. E. Haber, *Higgs Bosons in Supersymmetric Models. 1.*, *Nucl. Phys. B* **272** (1986) 1.
- [6] S. P. Martin, *A Supersymmetry primer*, *Adv. Ser. Direct. High Energy Phys.* **18** (1998) 1 [[hep-ph/9709356](#)].
- [7] D. J. Miller, R. Nevzorov and P. M. Zerwas, *The Higgs sector of the next-to-minimal supersymmetric standard model*, *Nucl. Phys. B* **681** (2004) 3 [[hep-ph/0304049](#)].
- [8] U. Ellwanger, C. Hugonie and A. M. Teixeira, *The Next-to-Minimal Supersymmetric Standard Model*, *Phys. Rept.* **496** (2010) 1 [[0910.1785](#)].
- [9] M. Maniatis, *The Next-to-Minimal Supersymmetric extension of the Standard Model reviewed*, *Int. J. Mod. Phys. A* **25** (2010) 3505 [[0906.0777](#)].
- [10] J.-J. Cao, Z.-X. Heng, J. M. Yang, Y.-M. Zhang and J.-Y. Zhu, *A SM-like Higgs near 125 GeV in low energy SUSY: a comparative study for MSSM and NMSSM*, *JHEP* **03** (2012) 086 [[1202.5821](#)].
- [11] J. Cao, Y. He, L. Shang, Y. Zhang and P. Zhu, *Current status of a natural NMSSM in light of LHC 13 TeV data and XENON-1T results*, *Phys. Rev.* **D99** (2019) 075020 [[1810.09143](#)].
- [12] J. Cao, Y. He, L. Shang, W. Su and Y. Zhang, *Natural NMSSM after LHC Run I and the Higgsino dominated dark matter scenario*, *JHEP* **08** (2016) 037 [[1606.04416](#)].
- [13] J. Cao, Y. He, L. Shang, W. Su, P. Wu and Y. Zhang, *Strong constraints of LUX-2016 results on the natural NMSSM*, *JHEP* **10** (2016) 136 [[1609.00204](#)].
- [14] Z. Heng, X. Gong and H. Zhou, *Pair production of Higgs boson in NMSSM at the LHC with the next-to-lightest CP-even Higgs boson being SM-like*, *Chin. Phys. C* **42** (2018) 073103 [[1805.01598](#)].
- [15] J. Cao, X. Guo, Y. He, P. Wu and Y. Zhang, *Diphoton signal of the light Higgs boson in natural NMSSM*, *Phys. Rev. D* **95** (2017) 116001 [[1612.08522](#)].
- [16] J. Cao, D. Li, L. Shang, P. Wu and Y. Zhang, *Exploring the Higgs Sector of a Most Natural NMSSM and its Prediction on Higgs Pair Production at the LHC*, *JHEP* **12** (2014) 026 [[1409.8431](#)].
- [17] U. Ellwanger, M. Muehlleitner, N. Rompotis, N. R. Shah and D. Winterbottom, *Benchmark Lines and Planes for Higgs-to-Higgs Decays in the NMSSM*, [2403.15046](#).
- [18] U. Ellwanger and C. Hugonie, *Benchmark planes for Higgs-to-Higgs decays in the NMSSM*, *Eur. Phys. J. C* **82** (2022) 406 [[2203.05049](#)].

- [19] S. Ma, K. Wang and J. Zhu, *Higgs decay to light (pseudo)scalars in the semi-constrained NMSSM*, *Chin. Phys. C* **45** (2021) 023113 [[2006.03527](#)].
- [20] W. Wang, M. Zhang and J. Zhao, *Higgs exotic decays in general NMSSM with self-interacting dark matter*, *Int. J. Mod. Phys. A* **33** (2018) 1841002 [[1604.00123](#)].
- [21] J. Cao, F. Ding, C. Han, J. M. Yang and J. Zhu, *A light Higgs scalar in the NMSSM confronted with the latest LHC Higgs data*, *JHEP* **11** (2013) 018 [[1309.4939](#)].
- [22] D. Curtin et al., *Exotic decays of the 125 GeV Higgs boson*, *Phys. Rev. D* **90** (2014) 075004 [[1312.4992](#)].
- [23] J. Cheng, R. Husain, L. Li and M. J. Strassler, *Limits on an Exotic Higgs Decay From a Recast ATLAS Four-Lepton Analysis*, [2412.14452](#).
- [24] H. Zhou and G. Ban, *Status of Z_3 -NMSSM featuring a light bino-dominated LSP and a light singlet-like scalar under the LZ Experiment*, [2502.14664](#).
- [25] S. Liu, Y.-L. Tang, C. Zhang and S.-h. Zhu, *Exotic Higgs Decay $h \rightarrow \phi\phi \rightarrow 4b$ at the LHeC*, *Eur. Phys. J. C* **77** (2017) 457 [[1608.08458](#)].
- [26] F. Domingo, S. Heinemeyer, J. S. Kim and K. Rolbiecki, *The NMSSM lives: with the 750 GeV diphoton excess*, *Eur. Phys. J. C* **76** (2016) 249 [[1602.07691](#)].
- [27] D. Curtin, R. Essig and Y.-M. Zhong, *Uncovering light scalars with exotic Higgs decays to $b\bar{b}\mu^+\mu^-$* , *JHEP* **06** (2015) 025 [[1412.4779](#)].
- [28] S. F. King, M. Mühlleitner, R. Nevzorov and K. Walz, *Discovery Prospects for NMSSM Higgs Bosons at the High-Energy Large Hadron Collider*, *Phys. Rev. D* **90** (2014) 095014 [[1408.1120](#)].
- [29] T. Liu and C. T. Potter, *Exotic Higgs Decay $h \rightarrow a_1 a_1$ at the International Linear Collider: a Snowmass White Paper*, in *Snowmass 2013: Snowmass on the Mississippi*, 8, 2013, [1309.0021](#).
- [30] J. Huang, T. Liu, L.-T. Wang and F. Yu, *Supersymmetric Exotic Decays of the 125 GeV Higgs Boson*, *Phys. Rev. Lett.* **112** (2014) 221803 [[1309.6633](#)].
- [31] J. Huang, T. Liu, L.-T. Wang and F. Yu, *Supersymmetric Subelectroweak Scale Dark Matter, the Galactic Center Gamma-Ray Excess, and Exotic Decays of the 125 GeV Higgs Boson*, *Phys. Rev. D* **90** (2014) 115006 [[1407.0038](#)].
- [32] J. Cao, F. Li, J. Lian, Y. Pan and D. Zhang, *Impact of LHC probes of SUSY and recent measurement of $(g-2)_\mu$ on Z_3 -NMSSM*, *Sci. China Phys. Mech. Astron.* **65** (2022) 291012 [[2204.04710](#)].
- [33] H. Zhou, J. Cao, J. Lian and D. Zhang, *Singlino-dominated dark matter in Z_3 -NMSSM*, [2102.05309](#).
- [34] XENON collaboration, E. Aprile et al., *Dark Matter Search Results from a One Ton-Year Exposure of XENON1T*, *Phys. Rev. Lett.* **121** (2018) 111302 [[1805.12562](#)].

- [35] PANDAX-II collaboration, Q. Wang et al., *Results of dark matter search using the full PandaX-II exposure*, *Chin. Phys. C* **44** (2020) 125001 [[2007.15469](#)].
- [36] PANDAX-II collaboration, X. Cui et al., *Dark Matter Results From 54-Ton-Day Exposure of PandaX-II Experiment*, *Phys. Rev. Lett.* **119** (2017) 181302 [[1708.06917](#)].
- [37] LZ collaboration, J. Aalbers et al., *First Dark Matter Search Results from the LUX-ZEPLIN (LZ) Experiment*, *Phys. Rev. Lett.* **131** (2023) 041002 [[2207.03764](#)].
- [38] LZ collaboration, J. Aalbers et al., *Dark Matter Search Results from 4.2 Tonne-Years of Exposure of the LUX-ZEPLIN (LZ) Experiment*, *Phys. Rev. Lett.* **135** (2025) 011802 [[2410.17036](#)].
- [39] K. Choi, S. H. Im, K. S. Jeong and C. B. Park, *Light Higgs bosons in the general NMSSM*, *Eur. Phys. J. C* **79** (2019) 956 [[1906.03389](#)].
- [40] J. Cao, X. Jia, L. Meng, Y. Yue and D. Zhang, *Status of the singlino-dominated dark matter in general Next-to-Minimal Supersymmetric Standard Model*, *JHEP* **03** (2023) 198 [[2210.08769](#)].
- [41] J. Cao, X. Jia and J. Lian, *Unified interpretation of the muon $g-2$ anomaly, the 95 GeV diphoton, and $b\bar{b}$ excesses in the general next-to-minimal supersymmetric standard model*, *Phys. Rev. D* **110** (2024) 115039 [[2402.15847](#)].
- [42] L. Meng, J. Cao, F. Li and S. Yang, *Dark Matter physics in general NMSSM*, *JHEP* **08** (2024) 212 [[2405.07036](#)].
- [43] J. Cao, D. Li, J. Lian, Y. Yue and H. Zhou, *Singlino-dominated dark matter in general NMSSM*, [2102.05317](#).
- [44] J. Cao, X. Jia, J. Lian and L. Meng, *95 GeV diphoton and $b\bar{b}$ excesses in the general next-to-minimal supersymmetric standard model*, *Phys. Rev. D* **109** (2024) 075001 [[2310.08436](#)].
- [45] J. Cao, J. Lian, Y. Pan, Y. Yue and D. Zhang, *Impact of recent $(g - 2)_\mu$ measurement on the light CP-even Higgs scenario in general Next-to-Minimal Supersymmetric Standard Model*, *JHEP* **03** (2022) 203 [[2201.11490](#)].
- [46] Y. Yue, J. Cao, F. Li and Z. Li, *Attractive features of Higgsino dark matter in the next-to-minimal supersymmetric standard model*, *Phys. Rev. D* **112** (2025) 095022 [[2503.10985](#)].
- [47] M. Pospelov, A. Ritz and M. B. Voloshin, *Secluded WIMP Dark Matter*, *Phys. Lett. B* **662** (2008) 53 [[0711.4866](#)].
- [48] S. Profumo, M. J. Ramsey-Musolf and G. Shaughnessy, *Singlet higgs phenomenology and the electroweak phase transition*, *Journal of High Energy Physics* **2007** (2007) 010.
- [49] J. Kozaczuk, M. J. Ramsey-Musolf and J. Shelton, *Exotic higgs boson decays and the electroweak phase transition*, *Phys. Rev. D* **101** (2020) 115035.

- [50] M. Carena, Y. Wang, M. Carena, Y. Wang, M. Carena and Z. Liu, *Electroweak phase transition with spontaneous z 2 -breaking*, *JOURNAL of HIGH ENERGY PHYSICS* **2020** (2020) .
- [51] M. Carena, J. Kozaczuk, Z. Liu, T. Ou, M. J. Ramsey-Musolf, J. Shelton et al., *Probing the Electroweak Phase Transition with Exotic Higgs Decays*, *LHEP* **2023** (2023) 432 [2203.08206].
- [52] CMS collaboration, A. Hayrapetyan et al., *Search for the decay of the Higgs boson to a pair of light pseudoscalar bosons in the final state with four bottom quarks in proton-proton collisions at $\sqrt{s} = 13$ TeV*, *JHEP* **06** (2024) 097 [2403.10341].
- [53] CMS collaboration, A. Hayrapetyan et al., *Search for exotic decays of the Higgs boson to a pair of pseudoscalars in the $\mu\mu bb$ and $\tau\tau bb$ final states*, *Eur. Phys. J. C* **84** (2024) 493 [2402.13358].
- [54] CMS collaboration, V. Khachatryan et al., *Search for light bosons in decays of the 125 GeV Higgs boson in proton-proton collisions at $\sqrt{s} = 8$ TeV*, *JHEP* **10** (2017) 076 [1701.02032].
- [55] ATLAS collaboration, M. Aaboud et al., *Search for Higgs boson decays into a pair of light bosons in the $bb\mu\mu$ final state in pp collision at $\sqrt{s} = 13$ TeV with the ATLAS detector*, *Phys. Lett. B* **790** (2019) 1 [1807.00539].
- [56] CMS collaboration, A. M. Sirunyan et al., *Search for an exotic decay of the Higgs boson to a pair of light pseudoscalars in the final state with two b quarks and two τ leptons in proton-proton collisions at $\sqrt{s} = 13$ TeV*, *Phys. Lett. B* **785** (2018) 462 [1805.10191].
- [57] ATLAS collaboration, G. Aad et al., *Search for decays of the Higgs boson into a pair of pseudoscalar particles decaying into $bb\tau^+\tau^-$ using pp collisions at $s=13$ TeV with the ATLAS detector*, *Phys. Rev. D* **110** (2024) 052013 [2407.01335].
- [58] ATLAS collaboration, G. Aad et al., *Search for Higgs boson decays into a pair of pseudoscalar particles in the $\gamma\gamma\tau_{had}\tau_{had}$ final state using pp collisions at $\sqrt{s} = 13$ TeV with the ATLAS detector*, **2412.14046**.
- [59] ATLAS collaboration, G. Aad et al., *Search for new light gauge bosons in Higgs boson decays to four-lepton final states in pp collisions at $\sqrt{s} = 8$ TeV with the ATLAS detector at the LHC*, *Phys. Rev. D* **92** (2015) 092001 [1505.07645].
- [60] CMS collaboration, S. Chatrchyan et al., *Search for a Non-Standard-Model Higgs Boson Decaying to a Pair of New Light Bosons in Four-Muon Final States*, *Phys. Lett. B* **726** (2013) 564 [1210.7619].
- [61] CMS collaboration, V. Khachatryan et al., *A search for pair production of new light bosons decaying into muons*, *Phys. Lett. B* **752** (2016) 146 [1506.00424].
- [62] ATLAS collaboration, M. Aaboud et al., *Search for Higgs boson decays to*

beyond-the-Standard-Model light bosons in four-lepton events with the ATLAS detector at $\sqrt{s} = 13$ TeV, *JHEP* **06** (2018) 166 [[1802.03388](#)].

- [63] CMS collaboration, A. M. Sirunyan et al., *A search for pair production of new light bosons decaying into muons in proton-proton collisions at 13 TeV*, *Phys. Lett. B* **796** (2019) 131 [[1812.00380](#)].
- [64] H. Bahl, T. Biekötter, S. Heinemeyer, C. Li, S. Paasch, G. Weiglein et al., *HiggsTools: BSM scalar phenomenology with new versions of HiggsBounds and HiggsSignals*, *Comput. Phys. Commun.* **291** (2023) 108803 [[2210.09332](#)].
- [65] U. Ellwanger, *NONRENORMALIZABLE INTERACTIONS FROM SUPERGRAVITY, QUANTUM CORRECTIONS AND EFFECTIVE LOW-ENERGY THEORIES*, *Phys. Lett. B* **133** (1983) 187.
- [66] S. A. Abel, *Destabilizing divergences in the NMSSM*, *Nucl. Phys. B* **480** (1996) 55 [[hep-ph/9609323](#)].
- [67] C. F. Kolda, S. Pokorski and N. Polonsky, *Stabilized singlets in supergravity as a source of the μ - parameter*, *Phys. Rev. Lett.* **80** (1998) 5263 [[hep-ph/9803310](#)].
- [68] C. Panagiotakopoulos and K. Tamvakis, *Stabilized NMSSM without domain walls*, *Phys. Lett. B* **446** (1999) 224 [[hep-ph/9809475](#)].
- [69] G. G. Ross and K. Schmidt-Hoberg, *The Fine-Tuning of the Generalised NMSSM*, *Nucl. Phys. B* **862** (2012) 710 [[1108.1284](#)].
- [70] H. M. Lee, S. Raby, M. Ratz, G. G. Ross, R. Schieren, K. Schmidt-Hoberg et al., *A unique \mathbb{Z}_4^R symmetry for the MSSM*, *Phys. Lett. B* **694** (2011) 491 [[1009.0905](#)].
- [71] H. M. Lee, S. Raby, M. Ratz, G. G. Ross, R. Schieren, K. Schmidt-Hoberg et al., *Discrete R symmetries for the MSSM and its singlet extensions*, *Nucl. Phys. B* **850** (2011) 1 [[1102.3595](#)].
- [72] G. G. Ross, K. Schmidt-Hoberg and F. Staub, *The Generalised NMSSM at One Loop: Fine Tuning and Phenomenology*, *JHEP* **08** (2012) 074 [[1205.1509](#)].
- [73] S. Baum, M. Carena, N. R. Shah and C. E. Wagner, *Higgs portals for thermal Dark Matter. EFT perspectives and the NMSSM*, *JHEP* **04** (2018) 069 [[1712.09873](#)].
- [74] ATLAS collaboration, G. Aad et al., *Search for heavy Higgs bosons decaying into two tau leptons with the ATLAS detector using pp collisions at $\sqrt{s} = 13$ TeV*, *Phys. Rev. Lett.* **125** (2020) 051801 [[2002.12223](#)].
- [75] ATLAS collaboration, G. Aad et al., *Search for charged Higgs bosons decaying into a top quark and a bottom quark at $\sqrt{s} = 13$ TeV with the ATLAS detector*, *JHEP* **06** (2021) 145 [[2102.10076](#)].
- [76] F. Staub, *SARAH*, [0806.0538](#).
- [77] F. Staub, *SARAH 3.2: Dirac Gauginos, UFO output, and more*, *Comput. Phys. Commun.* **184** (2013) 1792 [[1207.0906](#)].

- [78] F. Staub, *SARAH 4 : A tool for (not only SUSY) model builders*, *Comput. Phys. Commun.* **185** (2014) 1773 [[1309.7223](#)].
- [79] F. Staub, *Exploring new models in all detail with SARAH*, *Adv. High Energy Phys.* **2015** (2015) 840780 [[1503.04200](#)].
- [80] W. Porod and F. Staub, *SPheno 3.1: extensions including flavour, cp-phases and models beyond the mssm*, *Computer Physics Communications* **183** (2012) 2458–2469.
- [81] W. Porod, *SPheno, a program for calculating supersymmetric spectra, SUSY particle decays and SUSY particle production at e+ e- colliders*, *Comput. Phys. Commun.* **153** (2003) 275 [[hep-ph/0301101](#)].
- [82] G. Belanger, F. Boudjema and A. Pukhov, *micrOMEGAs : a code for the calculation of Dark Matter properties in generic models of particle interaction*, in *The Dark Secrets of the Terascale: Proceedings, TASI 2011, Boulder, Colorado, USA, Jun 6 - Jul 11, 2011*, pp. 739–790, 2013, [1402.0787](#), DOI.
- [83] F. Feroz, M. P. Hobson and M. Bridges, *MultiNest: an efficient and robust Bayesian inference tool for cosmology and particle physics*, *Mon. Not. Roy. Astron. Soc.* **398** (2009) 1601 [[0809.3437](#)].
- [84] G. A. et al. [ATLAS and CMS], *Combined Measurement of the Higgs Boson Mass in pp Collisions at $\sqrt{s} = 7$ and 8 TeV with the ATLAS and CMS Experiments*, *Phys. Rev. Lett.* **114** (2015) 191803 [[1503.07589](#)].
- [85] P. Bechtle, S. Heinemeyer, O. Stål, T. Stefaniak and G. Weiglein, *HiggsSignals: Confronting arbitrary Higgs sectors with measurements at the Tevatron and the LHC*, *Eur. Phys. J. C* **74** (2014) 2711 [[1305.1933](#)].
- [86] O. Stål and T. Stefaniak, *Constraining extended Higgs sectors with HiggsSignals*, *PoS EPS-HEP2013* (2013) 314 [[1310.4039](#)].
- [87] P. Bechtle, S. Heinemeyer, O. Stål, T. Stefaniak and G. Weiglein, *Probing the Standard Model with Higgs signal rates from the Tevatron, the LHC and a future ILC*, *JHEP* **11** (2014) 039 [[1403.1582](#)].
- [88] P. Bechtle, S. Heinemeyer, T. Klingl, T. Stefaniak, G. Weiglein and J. Wittbrodt, *HiggsSignals-2: Probing new physics with precision Higgs measurements in the LHC 13 TeV era*, *Eur. Phys. J. C* **81** (2021) 145 [[2012.09197](#)].
- [89] P. Bechtle, O. Brein, S. Heinemeyer, G. Weiglein and K. E. Williams, *HiggsBounds: Confronting Arbitrary Higgs Sectors with Exclusion Bounds from LEP and the Tevatron*, *Comput. Phys. Commun.* **181** (2010) 138 [[0811.4169](#)].
- [90] P. Bechtle, O. Brein, S. Heinemeyer, G. Weiglein and K. E. Williams, *HiggsBounds 2.0.0: Confronting Neutral and Charged Higgs Sector Predictions with Exclusion Bounds from LEP and the Tevatron*, *Comput. Phys. Commun.* **182** (2011) 2605 [[1102.1898](#)].

- [91] P. Bechtle, O. Brein, S. Heinemeyer, O. Stal, T. Stefaniak, G. Weiglein et al., *Recent Developments in HiggsBounds and a Preview of HiggsSignals*, *PoS CHARGED2012* (2012) 024 [[1301.2345](#)].
- [92] P. Bechtle, O. Brein, S. Heinemeyer, O. Stal, T. Stefaniak, G. Weiglein et al., *HiggsBounds – 4: Improved Tests of Extended Higgs Sectors against Exclusion Bounds from LEP, the Tevatron and the LHC*, *Eur. Phys. J. C* **74** (2014) 2693 [[1311.0055](#)].
- [93] P. Bechtle, D. Dercks, S. Heinemeyer, T. Klingl, T. Stefaniak, G. Weiglein et al., *HiggsBounds-5: Testing Higgs Sectors in the LHC 13 TeV Era*, *Eur. Phys. J. C* **80** (2020) 1211 [[2006.06007](#)].
- [94] PARTICLE DATA GROUP collaboration, P. Zyla et al., *Review of Particle Physics*, *PTEP* **2020** (2020) 083C01.
- [95] G. Belanger, F. Boudjema, A. Pukhov and A. Semenov, *MicrOMEGAs: A Program for calculating the relic density in the MSSM*, *Comput. Phys. Commun.* **149** (2002) 103 [[hep-ph/0112278](#)].
- [96] G. Belanger, F. Boudjema, C. Hugonie, A. Pukhov and A. Semenov, *Relic density of dark matter in the NMSSM*, *JCAP* **09** (2005) 001 [[hep-ph/0505142](#)].
- [97] G. Belanger, F. Boudjema, A. Pukhov and A. Semenov, *MicrOMEGAs 2.0: A Program to calculate the relic density of dark matter in a generic model*, *Comput. Phys. Commun.* **176** (2007) 367 [[hep-ph/0607059](#)].
- [98] G. Belanger, F. Boudjema, A. Pukhov and A. Semenov, *micrOMEGAs: A Tool for dark matter studies*, *Nuovo Cim. C* **033N2** (2010) 111 [[1005.4133](#)].
- [99] G. Belanger, F. Boudjema, A. Pukhov and A. Semenov, *micrOMEGAs_3: A program for calculating dark matter observables*, *Comput. Phys. Commun.* **185** (2014) 960 [[1305.0237](#)].
- [100] D. Barducci, G. Belanger, J. Bernon, F. Boudjema, J. Da Silva, S. Kraml et al., *Collider limits on new physics within micrOMEGAs_4.3*, *Comput. Phys. Commun.* **222** (2018) 327 [[1606.03834](#)].
- [101] G. Belanger, F. Boudjema, A. Goudelis, A. Pukhov and B. Zaldivar, *micrOMEGAs5.0 : Freeze-in*, *Comput. Phys. Commun.* **231** (2018) 173 [[1801.03509](#)].
- [102] PLANCK collaboration, N. Aghanim et al., *Planck 2018 results. VI. Cosmological parameters*, *Astron. Astrophys.* **641** (2020) A6 [[1807.06209](#)].
- [103] K. Griest and D. Seckel, *Three exceptions in the calculation of relic abundances*, *Phys. Rev. D* **43** (1991) 3191.
- [104] P. Athron, C. Balazs, A. Fowlie, G. Pozzo, G. White and Y. Zhang, *Strong first-order phase transitions in the NMSSM—a comprehensive survey*, *JHEP* **11** (2019) 151 [[1908.11847](#)].

[105] P. Athron, C. Balazs, A. Fowlie, L. Morris and L. Wu, *Cosmological phase transitions: From perturbative particle physics to gravitational waves*, *Prog. Part. Nucl. Phys.* **135** (2024) 104094 [[2305.02357](#)].

[106] <https://www.letpub.com.cn/>.